Pergamon

Geochemical dynamics of the Atlantis II Deep (Red Sea): II. Composition of metalliferous sediment pore waters

Pierre Anschutz,[1,]* Gérard Blanc,[1] Christophe Monnin,[2] and Jacques Boulègue[3]

[1]Université Bordeaux 1, Département de Géologie et Océanographie (D.G.O.) UMR CNRS 5805, 33405 Talence, France
[2]CNRS/Universite Paul Sabatier, Laboratoire de Geochimie, 38 rue des Trente-Six Ponts, 31400 Toulouse, France
[3]Université Pierre et Marie Curie (Paris 6), Géochimie et Métallogénie, CNRS UPRESA 7047, Tour.16/26, 5e ét., Boîte 0124, 4, Place Jussieu, 75252 Paris cedex 05, France

Abstract—The Atlantis II Deep is an axial depression of the Red Sea filled with highly saline brines and covered by layered metalliferous sediment. We report new data on the vertical distribution of major salts and trace metals dissolved in the pore waters of the metalliferous sediments. We have studied the chemical composition of interstitial waters of two sediment cores of the western (core 684) and southwestern (core 683) basins. The major dissolved elements are Na and Cl. Their concentrations are close to those of the brine overlying the sediment. The pore waters are undersaturated with respect to halite at the in situ conditions (62°C, 220 bars), but are saturated at the shipboard conditions (10°C, 1 bar). The salt and water contents of the bulk sediment show that core 683 contained halite in the solid fraction. A part of it precipitated after core collection, but most of it was present in situ. Thermodynamic calculations with a water–rock interaction model based on Pitzer's ion interaction approach reveal that equilibrium between the pore waters and anhydrite is achieved in sediment layers for which observations report the presence of this mineral. We used a transport model, which shows that molecular diffusion can smooth the profile of dissolved salt and partly erase the pore water record of past variations of salinity in the lower brine. For example, we calculated that the pore water record of modern variation of brine salinity is rapidly smoothed by molecular diffusion. The dissolved transition metals show large variations with depth in the interstitial waters. The profiles of core 683 reflect the possible advection of hydrothermal fluid within the sediment of the southwestern basin. The distribution of dissolved metals in core 684 is the result of diagenetic reactions, mainly the reduction of Mn-oxide with dissolved Fe(II), the recrystallization of primary oxide minerals, and the precipitation of authigenic Mn-carbonates. *Copyright © 2000 Elsevier Science Ltd*

1. INTRODUCTION

The Atlantis II Deep is the largest present-day ore-forming environment. It consists of a 60-km² topographic depression located in the axial trough of the Red Sea at 2000-m depth, which traps hot and dense brines that cover a 10–30-m-thick sequence of metalliferous sediment. The solid fraction of the sediment is of two different origins. The first is the normal Red Sea pelagic sediment, which consists of biogenic calcareous and/or siliceous components and silico-clastic detrital particles. In the Atlantis II Deep, this fraction is diluted by metalliferous sediment, which consists of metal oxides, sulphides, carbonates, sulphates, and silicates that precipitated from the hydrothermal fluids. The sediment lies on a young basaltic substratum. The bottom sediments were deposited between 28,000 and 23,000 yrs ago (Ku et al., 1969; Shanks III and Bischoff, 1980) except those of the southwestern part of the deep, which are about 6000 yrs old (Anschutz and Blanc, 1995a). Deposition of metalliferous sediment began ~15,000 yrs ago (Shanks and Bischoff, 1980) and the metalliferous fraction is dominant in the Holocene deposits, and minor below.

The metalliferous sediment mostly originates from hydrothermal fluids that have fed the brine pool (Zierenberg and Shanks, 1988; Anschutz et al., 1995). The composition of the sediment shows changes in vertical profiles that defined stratigraphic units (Bäcker and Richter, 1973; Anschutz and Blanc, 1995a). The depth variations of the mineralogical composition reflect temporal evolution of the physico-chemical conditions of the brine pool that resulted from changes in the composition, temperature, and flow rate of the hydrothermal fluid, and/or mixing event of the brine with seawater. The study of strontium isotope composition of the sediment showed, however, that a brine pool has persisted in the deepest parts of the depression since the beginning of the sedimentary history, and the Sr signature varied little during the Holocene period (Anschutz et al., 1995). New brines have supplied intermittently the deep and have changed the thickness of the brine pool (Bäcker and Richter, 1973).

The Atlantis II Deep is an active hydrothermal system, as demonstrated by the rising temperature from 54°C to 67.2°C of the bottom brine pool observed in the past 30 yrs (Monnin and Ramboz, 1996; Hartmann et al., 1998). It was deduced that during the 1966 to 1992 period, heat and salt were most likely to have been supplied by a hydrothermal solution with an average range of flow rate, temperature, and salinity of 670 to 1000 kg/s, 155°C to 310°C, and 270‰ to 370‰, respectively (Anschutz and Blanc, 1996).

Previous studies of Atlantis II Deep sediments, based on more than 600 cores collected from the deep (Bäcker and Richter, 1973), have defined five major environments and related processes of metalliferous particle precipitation, which are (Blanc et al., 1998): 1) the brine–seawater interface; 2) the

* Author to whom correspondence should be addressed (anschutz@geocean.u-bordeaux.fr).

anoxic brine; 3) the place of the hydrothermal fluid discharge; 4) veins; and 5) the layered sediment itself. The brine–seawater transition zone represents succession of a redox boundaries, which separate the anaerobic, dissolved metal-rich brine and the well oxygenated Red Sea bottom water (Danielsson et al., 1980; Hartmann, 1985). In 1992, this zone was 100-m thick and contained sharp interfaces between consecutively mixed brine layers of differing redox state and an upper zone of gradational changes (Blanc and Anschutz, 1995). Almost all the primary Fe(III) and Mg(III,IV) oxides and oxyhydroxides present in the sediment have precipitated in this transition zone due to oxidation of dissolved Fe(II) and Mn(II). Iron oxides are present as well crystallised minerals in the deepest layers and they consist of amorphous compounds in the most recent units. Iron oxides are abundant, which indicates that the brine pool generally did not contain sufficient dissolved reducing agent for Fe(III), such as hydrogen sulphide, to reduce all of the iron oxyhydroxide minerals that precipitated above the lower brine and settled into that layer (Anschutz and Blanc, 1995a). Manganese oxides are generally absent in the sediment pile, because dissolved Fe(II) is a reducing agent for these oxides. Mn-oxides are abundant in some layers, which must have been deposited in less reducing environments. Within the anoxic lower brine Fe(III) oxide could precipitate due to oxidation by manganese oxide formed in the overlying aerobic zone, that settles into the lower brine. Sulphide minerals are found in some stratigraphic units. They are sometimes co-deposited with iron oxides. Pottorf and Barnes (1983) showed that sulphide precipitation probably occurred both in the subsurface hydrothermal fluid as it ascended to the sea floor or upon or after discharge by cooling of the inflowing hot hydrothermal fluid due to mixing with the lower brine. Some coarse-grained sulphides have been transported into the deep by convective flow of the hydrothermal fluid (Pottorf and Barnes, 1983). It is also likely that anhydrite, which is abundant in some layers, precipitated by mixing of a calcium-rich hydrothermal fluid and the dissolved sulphate-bearing brine pool. The sediment of the southwestern basin contains veins that are filled with high-temperature sulphides and anhydrite (Zierenberg and Shanks, 1983; Pottorf and Barnes, 1983; Oudin et al., 1984; Missack et al., 1989). These veins are analogous to hydrothermal chimney precipitated on mid-oceanic ridges. The metalliferous sediment also undergoes diagenetic reactions, including recrystallization of amorphous phases, pore water–particle interactions, and authigenesis. Some studies focussed on metal oxide recrystallization (Bischoff, 1972; Badaut et al., 1990; Blanc et al., 1998, Schwertmann et al., 1998), but very little is known about the pore water composition and its relationship with the solid fraction, either in term of equilibrium, or in term of brine history.

The uppermost sediments from the Atlantis II Deep are muds containing up to 97% salty pore waters. Information about the chemical composition of interstitial waters is limited (Brooks et al., 1969; Hendricks et al., 1969; Manheim et al., 1974; Pushkina et al., 1982). Previous studies showed that the interstitial waters were as saline as the present-day lower brine and that the major dissolved elements varied little through the sediment column, whereas dissolved metals were generally enriched in pore waters in comparison with the brine pool.

The purpose of this paper is to describe the chemical composition of interstitial waters in Atlantis II Deep sediment cores that contain the whole sequence of metalliferous sediments. The study of interstitial waters is interesting in environments where the chemical conditions fluctuated markedly, because they may retain some of the composition of the buried water (e.g., Middelburg and DeLange, 1989). They allow distinctions to be made between the principal modes of solute transport, i.e., between diffusion and advection, and they provide the most sensitive indicators of the diagenetic reactions (Berner, 1980).

2. MATERIALS AND METHODS

Two cores of the southwestern basin (core 683; 16.2 m long) and western basin (core 684; 13.8 m long) were collected in 1985 during the "Hydrotherm" cruise of the RV Marion Dufresne (Blanc et al., 1986), using a 18-m-long Kühlenberg corer. Both cores reached the basaltic substratum and recovered the entire sedimentary sequence present at these sites. To our knowledge, these sediment cores have been the most studied among all those that have been collected in the Atlantis II Deep. They have been investigated for physical properties (Blanc et al. 1986; Anschutz and Blanc, 1993a), clay mineralogy (Badaut, 1988; Badaut et al., 1990; 1992), bulk mineralogy, and sediment chemistry (Blanc, 1987; Blanc et al., 1990; Anschutz, 1993; Anschutz and Blanc, 1995a,b; Blanc et al., 1998), organic matter content (Blanc et al., 1990), micropaleontology (Anschutz and Blanc, 1993b), and isotope geochemistry (Dupré et al., 1988; Anschutz et al., 1995; Blanc et al., 1995). The study of the solid fraction has allowed us to establish the sequence of deposit units. Core 684 consists in metal-enriched biodetritic sediments at the bottom (unit 1). This unit was deposited on a basaltic substratum from about −23000 B.P. to −11000 B.P. The overlying metalliferous sediment consists of two sulphide facies (units 2 and 4) separated by a Mn- and Fe-oxide-rich facies (unit 3). The substratum of the SW basin core is a basaltic rock ~6000 yrs old. Core 683 is divided into two units. At the bottom, unit L mainly contains Fe-oxides and anhydrite. From 1180 cm to the top, unit U contains sulphide minerals, poorly crystallized Fe-oxides and Fe-silicates. The stratigraphic correlation between the W and the SW basin deposits, and the sedimentation rates were estimated by the distribution of fossil foraminifera and pteropods (Anschutz and Blanc 1993b, 1995a).

The lithologic composition of core 684 can be compared readily to the lithostratigraphy proposed by Bäcker and Richter (1973) based on the study of hundreds of cores. The average thickness of the different facies calculated from several hundred of cores collected in the W, E, and N basins by the Preusag and the BRGM (Urvois, 1988) are close to the thickness of the corresponding units of core 684. The complete sedimentary series has rarely been recovered in the SW basin (Urvois, 1988). Therefore, the representativeness of core 683 cannot be estimated. Core 683 did not contain anhydrite and sulphide-filled veins as observed in several cores from the SW basin (Bäcker and Richter, 1973; Pottorf and Barnes, 1983; Zierenberg and Shanks, 1988). The presence of minerals such as magnetite or Mg-silicates at the bottom of the core has been interpreted as the result of the circulation of high-temperature fluids after the deposition of unit L sediment (Hackett and Bischoff, 1973; Zierenberg and Shanks, 1983).

The porosity of cores 683 and 684 remains above 90% in the upper 10 m of the sediment columns. The upper metre of sediment is very liquid, and the mud is soft but consolidated below. At the bottom of both cores, porosity decreases to about 60%. The decrease in porosity at the core bottom has been related to compaction and to the mineralogy of the solid particles (Anschutz, 1993). Interstitial water samples were collected by squeezing 10-cm-thick sediment slabs under nitrogen pressure (Reeburgh, 1967) within 24 h after the recovery of the cores. Despite the short time elapsed between coring and sediment sampling, the in situ temperature and pressure conditions could not be maintained during sediment processing. The mean pressure of the Altantis II Deep bottom is 220 bars and the temperature of the brine was about 62°C in 1985. The pore waters were extracted in the cold laboratory of the ship, at 1 bar and 10°C. The overlying brine was sampled at the coring site with 12-L Niskin bottles. The pore waters and Niskin bottle samples were filtered through 0.45-μm filters, acidified and stored in the dark at 4°C in pre-washed polypropylene bottles before analysis.

Concentration of dissolved metals (Ca, Mg, Sr, Rb, Fe, Mn, Zn, Cu,

and Cd) were measured within a few weeks after the cruise by atomic absorption using a Hitachi 7000 spectrometre (Tokyo, Japan) with Zeeman background correction. The concentrations were generally high enough to be determined from the linear portion of a calibration curve on sample diluted with Milli-Q water. NH_4NO_3 was used as a matrix modifier. Na and K were measured by atomic emission spectrometry. Sulphate was determined by ion chromatography, and Cl was determined by potentiometric titration with an Ag/Ag_2S electrode. Boron was measured by inductively coupled plasma-emission spectrometry. The precision was better than 1% for Cl, 2% for other major elements, and 10% for trace metals. The sum of charges showed a mean shift of 3.3% relative to electroneutrality. Correction was made on Na^+ concentration to obtain electroneutrality.

The total dissolved salt (TDS) of pore water samples was compared to independent measurements of the proportion of water, salt, and salt-free particles in sediments collected approximately every 50 cm. About 5 mL of sample were collected just after core recovery and were stored at 4°C in sealed glass bottles. Phase proportions were obtained by successive weighing of bulk mud, dried sediment, and washed and dried sediment kept in the same container at each stage.

3. RESULTS

The concentration of dissolved species in the free brine was obtained from samples collected above the two sites of coring. The results (Table 1) are identical for the two samples within 1% for major elements (10% for Mg) and 10% for minor solutes. This indicates that the brine is well mixed. Only Cd showed an important difference, with concentrations of 508 nmol/L at station 683 and 202 nmol/L at station 684. The pH and alkalinity of the brine were corrected for the in situ temperature from shipboard measurements (Blanc et al., 1986). The values are 5.8 and 0.839 meq/L, respectively. The TDS is close to previously reported values (Brewer and Spencer, 1969; Pushkina et al., 1982; Danielsson et al., 1980; Hartmann, 1985). It is slightly higher, in agreement with the regular increase of salinity of the brine observed from 1966 to 1992 (Anschutz and Blanc, 1996). Minor solutes, and particularly dissolved trace metals, showed large differences with the data collected in 1976 (Danielsson et al., 1980), which were also different from samples collected in 1966 (Brooks et al., 1969). This shows that during period of hydrothermal activity in the Atlantis II Deep the metal concentrations can change in the short time scale (less than 10 yrs), whereas major dissolved components fluctuate slowly. We cannot exclude that the trend we observed for some trace metals could be artefacts, due to the use of different analytical techniques.

The pore water concentrations of the major dissolved elements, such as the alkali, the alkaline earth, and chloride showed little variation within the cores. They were close to those of the free brine that covers the sediment. The average TDS of pore waters was 315 ± 8 g/L, which was the same value as the overlying brine pool. Na and Cl represented 97% of the TDS. Samples 683-14 and 683-15 had the lowest values (297 g/L) due to lower concentrations of all the major solutes. The volume of pore waters extracted from these samples was low (a few mL) due to the low porosity and the rapid obstruction of the squeezer by the small plate-shaped anhydrite. Therefore, an eventual small contamination of the squeezer with a few drops of rinsing water, or more probably dilution of the sample with the ultrapure nitric acid used for sample preservation could have affected the measurements. Due to this uncertainty, the composition of these samples will not be discussed further. A sample from the top of core 684 was suspected to

have been contaminated with seawater during core recovery and was also discarded.

The total dissolved solid content measured on the interstitial waters ($TDS/H_2O_{(IW)}$) was compared to the same ratio measured directly from sediment ($TDS/H_2O_{(S)}$) by weighing bulk, dried, and desalted samples. $TDS/H_2O_{(IW)}$ was calculated from the measured total dissolved load in volume unit (TDS_V in g/L), using the density ρ of the solutions according to:

$$TDS/H_2O_{(IW)} = TDS_V/(\rho - TDS_V)$$

The density of the interstitial brines at laboratory conditions (25°C, 1 bar) has been calculated with the computer code VOPO (Monnin, 1989). The mean value is 1203 kg/m^3. Since the pore water salinity does not change markedly along the cores, the value of $TDS/H_2O_{(IW)}$ is relatively constant, with values between 0.345 and 0.362 (Fig. 1). The values of $TDS/H_2O_{(S)}$ in the upper 11 m of core 684 are also close to the values of $TDS/H_2O_{(IW)}$, indicating that all the salt measured by weighing comes from the pore water. Below 11 m, $TDS/H_2O_{(S)}$ reaches values as high as 0.52, whereas $TDS/H_2O_{(IW)}$ remains at 0.355 (Fig. 1). This indicates that the sediment contains more salt than that dissolved in pore waters, and it suggests that halite was present in this sediment layer. The values of $TDS/H_2O_{(S)}$ of core 683 were higher than the ratio for pore waters. They increase regularly from the top to the bottom with values between 0.371 and 0.477. This suggests that almost the whole core 683 contained halite in the solid fraction.

The average Cl and Na concentrations in pore waters are 5.39 and 5.01 mol/L, respectively (Fig. 2). This is 8 to 9 times higher than the Red Sea bottom seawater (0.634 and 0.547 mol/L). Similarly, K, Ca, Sr, and B show only small variations along the vertical pore water profiles, but the differences are significant. For example, Ca values range between 120 and 140 mmol/L, with the lowest values in the samples of Mn-oxide-rich units of core 684. They are higher than seawater concentration. However, the enrichment factor is specific for each element. The Mg concentrations are between 29.7 and 35.4 mmol/L, whereas Red Sea water content is 60.1 mmol/L. Sulphate concentrations range from 6.6 to 10.6 mmol/L. This range is relatively larger than that for other major species. The highest value of dissolved sulphate occurred in sediment samples containing anhydrite ($CaSO_4$) in the solid fraction. Concentrations are close to the lower brine value (8.89 mmol/L), but as for Mg, they are lower than seawater (33.5 mmol/L). The depletion of Mg and SO_4 in oceanic hydrothermal waters is characteristic of waters that have reacted with hot basaltic substratum (Von Damm, 1990). The interaction of the solutions that generated the Atlantis II Deep brine with the oceanic crust has been confirmed by the study of the Sr isotopes (Zierenberg and Shanks, 1986; Anschutz et al., 1995; Blanc et al., 1995).

The dissolved transition metals show much greater variations along the pore water profiles (Fig. 2). The concentrations are compared to the whole-rock metal content (Anschutz and Blanc, 1995a). Dissolved iron and manganese are in the millimolar range in the interstitial waters and in the overlying brine pool. Iron concentration is the highest (up to 2 mmol/L) in unit U of core 683. The concentrations decrease steadily below a depth of 6 m to a concentration of about 0.33 mmol/L in unit L. The shape of the manganese profile is approximately the

Table 1. Chemical composition of interstitial waters, lower brines (H6 and H12), and Red Sea bottom water of cores 683 and 684 and calculated densities (d) and ionic strength (I).

| Name	Depth (cm)	Na mmol/l	K mmol/l	Ca mmol/l	Mg mmol/l	Cl mmol/l	SO4 mmol/l	B mmol/l	Fe mmol/l	Mn mmol/l	Sr mmol/l	Zn μmol/l	Cu μmol/l	Pb μmol/l	Cd nmol/l	TDS g/l	d 1bar, 25°	I
683																		
H6	—	4 987	59.0	138	29.2	5 370	8.89	0.849	1.17	1.77	0.684	81	0.08	23.9	508	314.6	1.2027	6.269
1	10	4 869	58.5	132	34.1	5 250	8.70	0.838	0.94	1.09	0.691	893	16.60	17.0	857	307.5	1.1983	6.114
2	115	5 018	58.5	131	35.0	5 400	8.51	0.838	1.89	1.27	0.705	538	19.10	16.3	1 020	316.2	1.2035	6.307
3	280	5 131	58.5	135	35.4	5 520	9.60	0.843	1.93	1.31	0.722	507	17.00	15.0	803	323.4	1.2080	6.470
4	320	5 089	57.9	133	32.8	5 470	8.71	0.858	1.90	1.30	0.705	447	7.56	15.6	714	320.4	1.2065	6.395
5	425	5 031	58.3	134	30.5	5 410	8.71	0.869	1.97	1.29	0.725	417	6.17	14.1	544	316.9	1.2042	6.317
6	530	5 008	57.2	130	32.1	5 380	9.00	0.830	1.85	1.27	0.714	337	5.65	13.9	534	315.2	1.2031	6.277
7	667	5 063	57.9	132	32.1	5 440	7.80	0.880	1.16	1.21	0.722	331	2.33	14.1	371	318.5	1.2053	6.350
8	733	4 893	57.4	133	32.8	5 270	9.30	0.818	1.19	1.20	0.712	257	4.96	13.8	521	308.8	1.1990	6.141
9	833	5 017	58.3	123	30.5	5 370	8.91	0.822	0.99	1.16	0.705	100	1.82	13.9	251	314.7	1.2028	6.253
10	923	4 988	58.5	132	31.7	5 360	9.80	0.827	0.77	1.14	0.707	67	0.64	14.8	76	314.1	1.2024	6.254
11	1 053	5 011	58.5	134	33.8	5 390	9.91	0.840	0.47	1.09	0.731	65	0.38	12.5	86	315.8	1.2035	6.297
12	1 133	5 055	59.0	133	32.8	5 430	10.30	0.736	0.60	1.08	0.722	96	1.20	16.4	395	318.3	1.2051	6.348
13	1 203	5 030	59.7	129	33.8	5 400	9.91	0.782	0.34	1.09	0.724	46	1.21	17.1	159	316.5	1.2039	6.304
16	1 513	5 042	61.3	139	32.8	5 430	10.60	0.784	0.33	1.09	0.722	37	0.06	16.7	49	318.3	1.2051	6.355
684																		
H12	—	4 992	59.0	138	31.8	5 380	8.99	0.847	1.18	1.55	0.696	78	0.08	23.7	202	315.2	1.2031	6.285
2	195	4 909	58.7	129	31.7	5 280	7.80	0.878	0.88	1.44	0.783	230	0.33	19.8	247	309.2	1.1993	6.143
3	420	5 089	59.0	122	29.7	5 440	8.40	0.773	0.05	1.54	0.847	214	0.59	20.7	173	318.7	1.2054	6.338
4	485	5 099	59.6	133	31.7	5 480	7.60	0.785	0.04	2.49	0.820	285	0.74	20.1	490	320.9	1.2068	6.402
5	555	5 012	59.0	128	30.5	5 380	7.80	0.634	0.04	2.45	0.820	260	1.12	19.9	623	315.1	1.2030	6.268
6	655	5 004	58.5	130	32.8	5 380	8.00	0.705	0.19	2.61	0.820	141	0.44	18.2	417	315.0	1.2030	6.273
7	853	5 088	58.3	121	29.7	5 440	7.40	0.759	0.10	2.47	0.786	95	0.23	14.5	338	318.6	1.2053	6.334
8	906	4 985	58.5	123	29.7	5 340	7.60	0.692	0.04	2.19	0.752	165	0.37	18.6	806	312.8	1.2015	6.209
9	1 031	4 990	57.4	134	32.1	5 370	8.40	0.759	0.29	2.42	0.759	37	0.08	14.4	593	314.5	1.2027	6.266
11	1 141	5 013	55.7	138	34.1	5 400	9.63	0.756	0.39	2.18	0.727	31	0.32	14.8	211	316.3	1.2038	6.315
12	1 234	5 008	58.7	125	30.8	5 370	6.81	0.771	0.43	1.53	0.697	43	0.05	17.1	317	314.4	1.2026	6.247
13	1 271	4 993	56.1	136	34.1	5 380	7.00	0.754	0.44	1.40	0.707	31	0.07	13.7	862	314.8	1.2028	6.276
14	1 300	4 957	54.5	131	32.8	5 330	7.00	0.670	0.38	1.10	0.707	43	0.36	12.0	145	311.9	1.2010	6.205
15	1 331	4 990	52.8	134	34.1	5 370	6.60	0.651	0.31	1.13	0.697	43	0.72	10.3	646	314.1	1.2024	6.259
seawater		547	11.8	11	60.1	634	33.50	0.482	—	—	0.126	—	—	0.1	—	40.6	1.0287	0.815
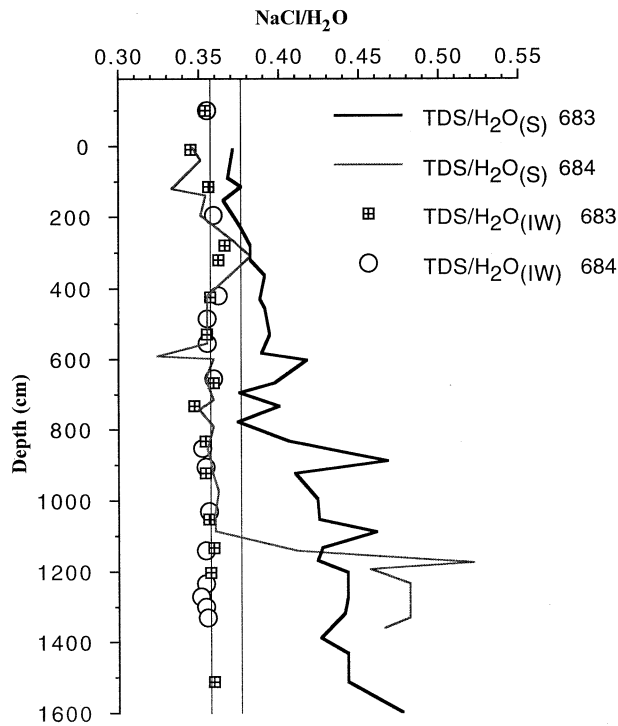
Fig. 1. Vertical profiles of the ratio between salt and H_2O in the bulk sediment (lines) and the extracted pore waters (symbols) for core 683 and 684. The symbols located above the 0 depth are for the overlying free brine. The vertical lines at $NaCl/H_2O = 0.357$ and 0.376 correspond to the ratio for the solubility of halite in water at the shipboard conditions (10°C, 1 bar) and in situ conditions (62°C, 220 bars), respectively.

same, but with a smaller concentration range (max = 1.31 mmol/L; min = 1.08 mmol/L). Fe concentrations are the lowest in unit 3 of core 684, especially in the subunits enriched in Mn-oxide (<0.053 mmol/L). Dissolved Mn concentrations of core 684 are close to the brine pool value in units 4 and 1, but they are higher (>2 mmol/L) in the units 2 and 3.

The upper part of core 683 contains more dissolved Zn, Cu, and Cd than core 684, and values are up to one order of magnitude higher than the overlying brine. In core 683 the concentrations decrease downward to values lower than those for the brine. The profiles are scattered in core 684, but all these metals show higher values in the subunits that contain Mn-oxides. Dissolved reduced sulphur has not been analysed, but neither the brine samples nor the sediment smelled of H_2S during the core and the Niskin bottle recovery, indicating very low concentrations of free H_2S.

The concentration of elements dissolved in pore waters is not obviously related to the concentrations in the solid fraction. The content of dissolved metals decreases in unit U of core 683, whereas particulate metals remain at high concentrations within this unit. The low concentration of dissolved Zn, Cu, and Cd in unit L agrees with the low particulate content. However, these metals are abundant in epigenetic features, which have been described for sediments of the same facies of the SW basin (Pottorf and Barnes, 1983). The concentrations of dissolved Mn are close to the concentration of the lower brine in core 683 and the upper 4 m of core 684. In these sediments, dissolved Mn is

in contact with variable amount of particulate Mn, which is present only as Mn(II) particles (Anschutz and Blanc, 1995a). The concentration is higher in pore water when dissolved Mn is in contact with Mn(III,IV) oxides of unit 3. The concentrations of dissolved Fe in core 684 are the lowest in unit 3, where Mn-oxides dominate the particulate fraction.

4. DISCUSSION

4.1. Dissolved major salts

The measured pore water salinity shows little variation with depth, and the concentrations are close to the values obtained for the overlying brine. This could suggest that the salinity of the pore waters results from past periods of sedimentation during which the mean salinity of the brine pool was the same as the present-day, or that the past variations were significant, but they have been smoothed by diffusion. This must be checked with a diffusion model. However, we showed that all of core 683 and a part of core 684 contained more salt than that dissolved in pore waters, suggesting that halite was present. Therefore, the uniform pore water salinity may simply reflect equilibrium with halite. By extension, solutes other than Na and Cl may also be controlled by mineral solubility. We have tested these hypotheses, first by calculating the saturation state of the Atlantis II Deep pore waters with respect to different salts and, secondly, by comparison to a molecular diffusion model.

4.1.1. Saturation index calculation

In order to test an eventual control of the pore water composition by equilibrium with solid phases, we have compared the ionic activity product (Q) of the solutes to the solubility product (K) of Na, Cl, Ca, Mg, SO_4, and K-bearing minerals. The saturation index (SI) is defined as the ratio of the ionic product to the solubility product (Q/K). Equilibrium is assumed when the SI of a given mineral is between 0.9 and 1.1 (see Monnin and Ramboz, 1996 or Monnin, 1999 for discussion). Details of the model are given in Monnin (1999).

The saturation indexes of halite and calcium sulphates (anhydrite and gypsum) have been calculated for both the in situ conditions and those that reach the sediment at the laboratory condition a few hours after core recovery, at the time of sampling the interstitial water. In 1985, when the cores were collected, the temperature of the lower brine pool was 62°C. We assume that the temperature in the sediment column was constant, even though temperature differences of about 6°C have been reported from direct measurements in 1966 (Erickson and Simmons, 1969). The SI profiles vs. depth are presented in Figure 3.

Ionic strength of interstitial waters is 6.28 ± 0.18 and it does not vary a lot along the studied profiles. This value is also equivalent to the ionic strength of the lower brine (6.28). The values of $TDS/H_2O_{(S)}$ suggest that at shipboard laboratory conditions the pore waters should be at equilibrium with halite in the major part of core 683 and at the bottom of core 684. However, the pore waters are undersaturated with halite at the in situ conditions (Fig. 3). This implies that the pore waters of the halite-bearing samples contained about 0.3 mol/kg H_2O more Na and Cl than what we have measured. This corresponds to the difference between the solubility of NaCl at 10°C and 1

(a)   Core 683
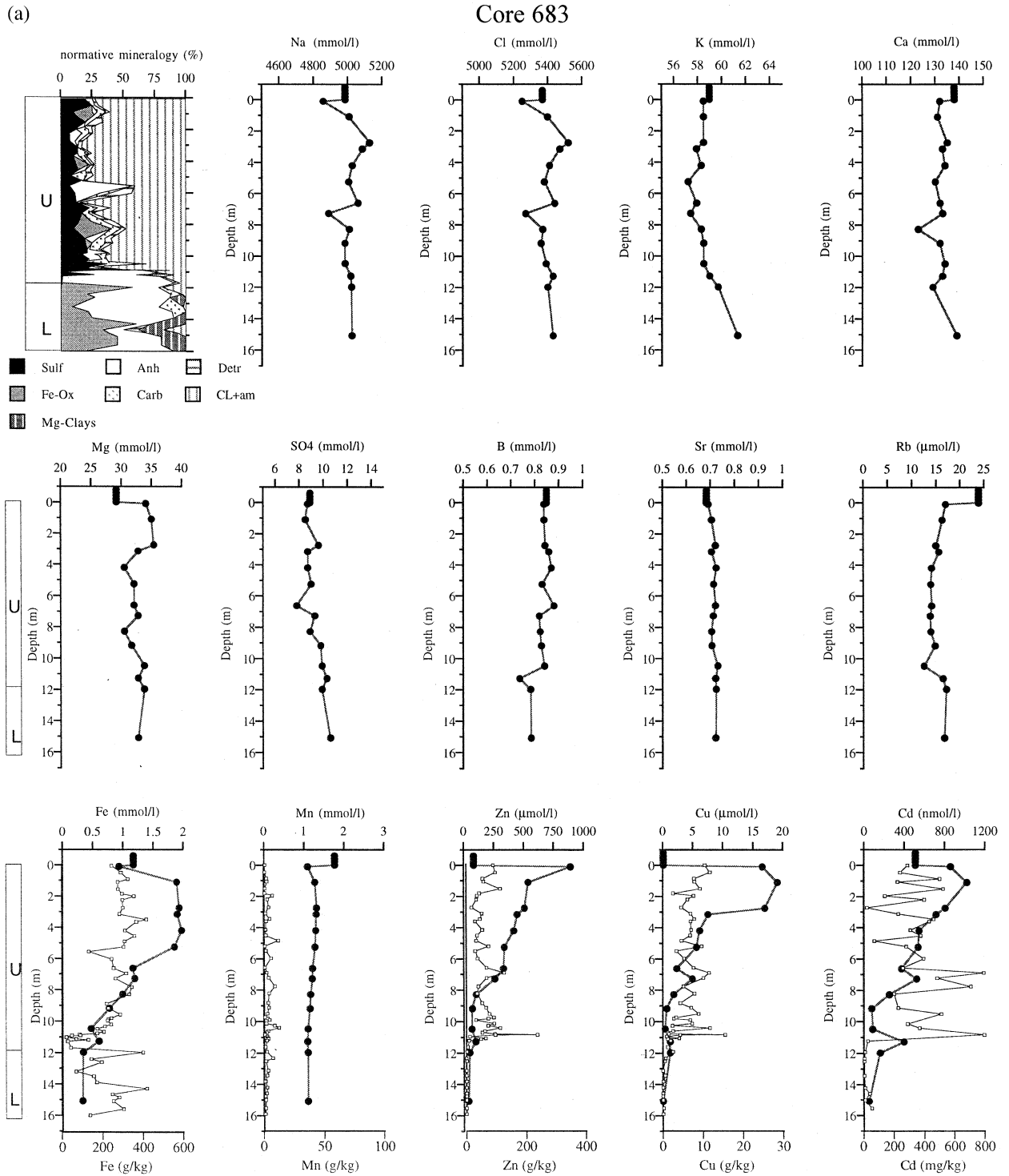
Fig. 2. Vertical profiles of major elements and some minor metals dissolved in pore waters from the two studied cores of the Atlantis II Deep. The profiles are compared to the distribution of minerals vs. depth, expressed as weight percent of dry, salt-free sediments. Sulf: Sulphide minerals; Fe-Ox: Fe-oxide and oxyhydroxide; Mn-Ox: Mn-oxide and oxyhydroxide; Anh: Anhydrite; Carb: Carbonates; Detr: Detrital silicates; CL+am: Clay minerals and amorphous Fe- and Si-compounds; Mg-CL: Magnesian phyllosilicates. The concentration of particulate transition metals (small square) is reported from Anschutz and Blanc (1995). The grey areas of the particulate Mn profile of core 684 correspond to the layers where Mn occurs mostly as Mn(III,IV) oxides. Else, it is present as Mn(II)-carbonates.

(b)   Core 684
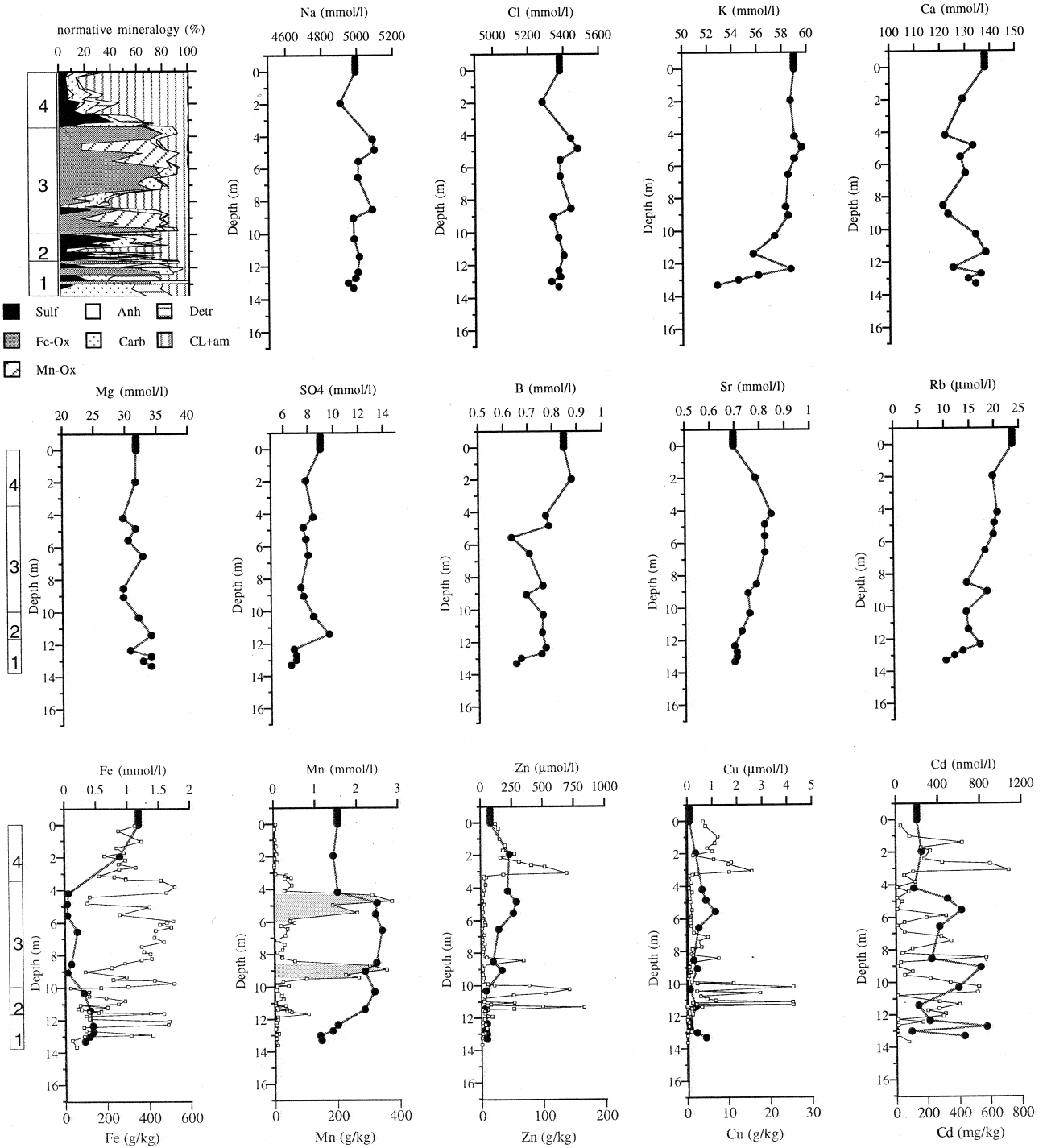
Fig. 2. Continued

bar and that at 62°C and 220 bars. This amount of halite (0.3 mol/kg) probably precipitated shortly after core collection because the pore waters became oversaturated at the surface conditions.

Anhydrite is slightly undersaturated at the in situ conditions (Fig. 4). The saturation index is highest in samples where

anhydrite is found. This suggests that Ca and sulphate concentrations are not controlled by equilibrium with anhydrite for most of core 684 and for unit U of core 683. However, when calculations are made using the corrected Na and Cl concentrations for halite-bearing sample, i.e., when 0.3 mol/kg H_2O of Na and Cl are added to the measured concentrations, the Q/K
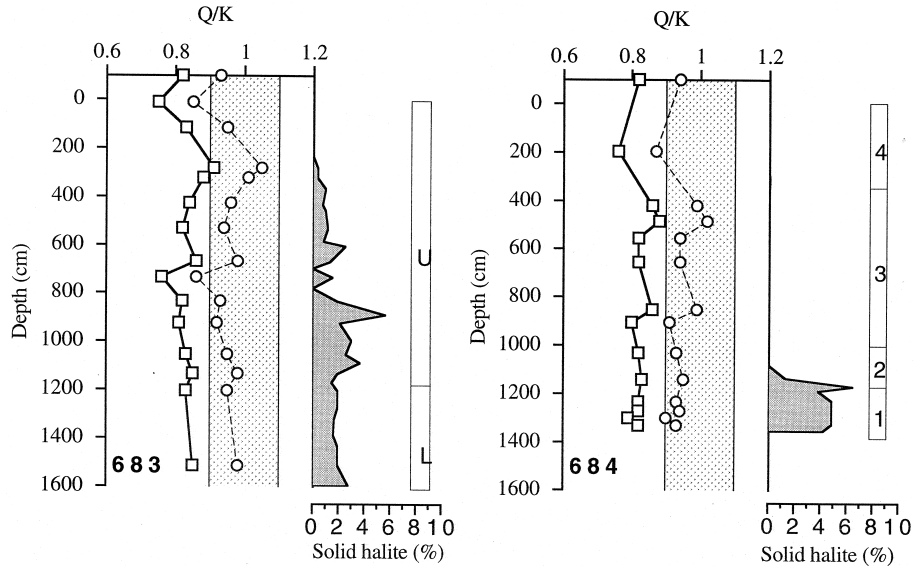
Fig. 3. Saturation state of pore waters with respect to halite at in situ conditions (squares) and at the condition of pore water sampling in the wet laboratory of the ship (circles), calculated with the code QSURK. The domain for thermodynamic equilibrium is between Q/K = 0.9 and Q/K = 1.1. The concentration of particulate halite present in the sediment (% of bulk sediment) is reported and has been calculated from the proportion of salt and water in sediments.

of anhydrite increases by about 0.06. This brings most of the pore waters collected from anhydrite-bearing intervals closer to equilibrium with this mineral. Core intervals that did not contain anhydrite, but contain halite, such as the bottom unit of core 684, remain undersaturated after the correction (Fig. 4).

4.1.2. Salt transport model for Atlantis II deep

We used a diffusion model to illustrate the possible magnitude of the effects on pore water composition of recent changes

in lower brine salinity. This model is based on the mathematical formulation described in detail by Lerman and Jones (1973). At time $t = 0$ we chose different compositions for the brine (C_B) and for the interstitial waters (C_{IW}):

$$\text{at } t = 0: (C_B) = (C_{0B}) \quad \text{and} \quad (C_{IW}) = (C_{0IW})$$

The concentration of a given element at the sediment–water interface ($z = 0$) is the same as its the concentration in the brine pool:
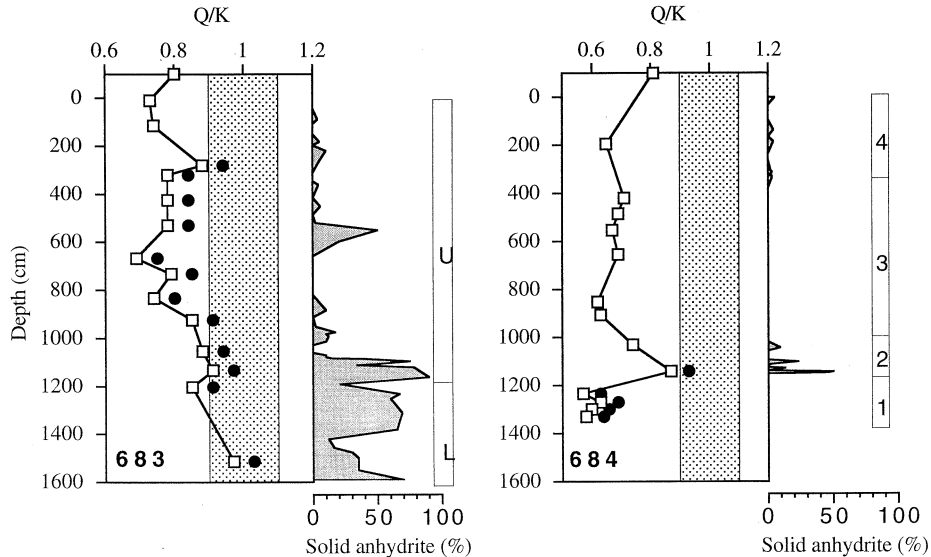

Fig. 4. Saturation state of pore waters with respect to anhydrite at in situ conditions (squares), calculated with the code QSURK. Black circles represents the corrected saturation state of anhydrite, when the Na and Cl content of halite-bearing sample corresponds to the saturation of pore waters with respect to halite. The concentration of particulate anhydrite present in the sediment (% solid fraction) is reported and has been determined by X-ray diffraction and chemical analysis of the sediment (Anschutz and Blanc, 1995a).

at $t = 0$: at $z = 0$, $C_{IW} = C_B$.

The sediment–water interface is taken as the origin ($z = 0$), and z is the depth in the sediment with positive values downward. The sedimentation rate U (in height per unit time) corresponds to a rate of pore water flow up ($U < 0$). The concentration of the brine pool is the algebraic sum of the flux of salt across the sediment–water interface, the accumulation of sediment, and a salt input from a hydrothermal fluid with a flux Q:

At $t > 0$ and at $z = 0$

$$H(dC_B/dt) = Q + D(\partial C_{IW}/\partial z)_{z = 0} - UC_{B\,z = 0}$$

where H is the mean thickness of the brine pool (in metres) and D is the diffusion coefficient in interstitial brine. The differential equation based on Fick's second law of diffusion describing the concentration of interstitial brine as a function of time (t) and position (z) is:

$$\partial C_{IW}/\partial t = D(\partial^2 C_{IW}/\partial z^2) - U(\partial C_{IW}/\partial z)$$

The solution of this equation is given by Lerman and Jones (1973) for the initial and boundary conditions given above. The diffusivity of an aqueous species D is calculated from the tracer diffusion coefficient given by Li and Gregory (1974), corrected for the temperature, viscosity, and mutual ion effect as described in detail in Anschutz et al. (1999). As the concentration increases, D can also vary according to a thermodynamic term (Felmy and Weare, 1991), which takes into account the activity coefficient of the solute. However, for a NaCl solution, such as the Atlantis II Deep brines, the overall effect of this term is less than 8% (Lasaga, 1979). Finally, D is corrected for porosity according to Boudreau (1996). The sedimentation rate was estimated at 1 mm/yrs for core 684 and 3 mm/yrs for core 683 (Anschutz and Blanc, 1995a). We have tested how fast molecular diffusion can smooth the profile of dissolved salt and partly erase the pore water record of past variations of salinity in the lower brine. The examples we have used to estimate the impact of diffusion are based on the recent evolution of brine salinity.

The salt budget for the period 1966 to 1992 was recently calculated for the Atlantis II deep (Anschutz and Blanc, 1996). It was deduced that the deep was fed by a hydrothermal solution, which supplied salt at a rate of 250 kg/s to 350 kg/s. Extrapolating back in time, this study showed that current hydrothermal activity began in the 30s. The part of salt flux that entered directly into the lower brine was 41 kg/s (Anschutz et al., 1998). This corresponds to a flux of 1.4×10^{-2} mmol/m²/s. Considering a mean thickness of this brine layer of 60 m for this period, we deduced that the concentration of chloride was 5000 mmol/L in 1935. The results depicted in Figure 5 are obtained for an initial chloride concentration in the pore waters of 5380 mmol/L and a Cl content of the free brine increasing from 5000 mmol/L in 1935 to the value measured in 1985 (5370 mmol/L). It is shown that the minimum value recorded in the pore water profile is located at 1.30 m and is 5300 mmol/L, far from the initial value of 5000 mmol/L. We have also simulated a longer period of low salinity, using the same initial conditions, but a lower flux (1.5×10^{-3} mmol/m²/s) and a longer time (500 yrs). Here again the minimum is at 5300 mmol/L, and is located at 4.2-m depth. Both examples show that important fluctuations of concentration in the brine are
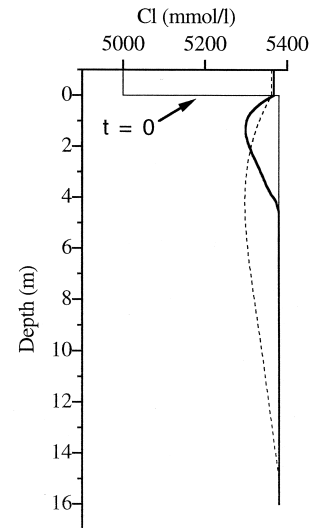

Fig. 5. Simulation for the chloride profile when the initial concentration in pore waters is 5380 mmol/L, and the overlying brine concentration increases from 5000 mmol/L to 5370 mmol/L during 50 years (Q = 0.014 mmol/m²/s; full line), or during 500 yrs (Q = 0.0015 mmol/m²/s; dotted line). The simulated sedimentation rate is 1 mm/yrs.

greatly smoothed by molecular diffusion in the buried water. We can then conclude that the relative constancy of pore water Cl concentration does not indicate that the salinity of the overlying brine has not or little changed. The concentrations may have fluctuated around a mean value, which is close to the present-day value, but the oscillations have not been recorded.

4.2. Dissolved Metals

The distribution of dissolved transition metals is much more variable along the pore water profiles than the distribution of major species. The shape of the profiles can be interpreted in term of solute transport, or in term of diagenetic reaction or equilibrium with the solid fraction. Unfortunately, the saturation index for metalliferous minerals cannot be precisely calculated because the thermodynamic properties of such solutes in concentrated multi-component solutions at high T and P is beyond the capacities of current models. Also, most of the minerals that occur in the Atlantis II Deep are poorly crystallized phases for which thermodynamic data are not accurately known. Therefore, a quantitative approach of pore water–mineral interactions is not possible for dissolved transition metals. Nevertheless, some abrupt changes in the pore water profile of core 684 can be qualitatively interpreted as the result of diagenetic reactions as discussed in the next section.

Pore water distribution of Fe, Zn, Cu, and Cd in core 683 show smooth-shaped profiles, from high values at the top grading to low values in unit L at the bottom of the core. The concentrations at the top of the core are above those of the overlying brine pool. Considering that the pore water metal content has retained some of the composition of the buried brine, the high values we measured at the top indicate that the metal concentrations in the brine could have been higher in the past than in 1985. However, the western basin where core 684 is located, is well connected to the southwestern basin (core

683). Historical observations and theoretical considerations indicate that the lower brine was a homogeneous, convectively mixed layer (Turner, 1969; Voohris and Dorson, 1975; Anschutz et al., 1998). Therefore, what we observe at the top of core 683 should be seen at the top core 684, which is not the case. A separation of the brines that overlaid the two stations in the recent past is not realistic.

There are more obvious reasons for the observed differences between core 683 and 684. It is well established that the hydrothermal fluid that feed directly the lower brine is discharging into the SW basin where core 683 was collected (Bäcker and Richter, 1973; Hartmann, 1973; Zierenberg and Shanks, 1988). The difference in stratigraphy between the sediment of the SW basin and the cores collected in other basins is a direct consequence of this. Core 683 shows clearly the metasomatic effects of inflow of high-temperature hydrothermal fluid at depth including recrystallization of metalliferous sediment and precipitation of magnetite and Mg-rich silicates. These minerals are absent in the other basins on the Atlantis II Deep (Bäcker and Richter, 1973). Anhydrite present in sediment of the SW basin preserves a fluid-inclusion record of the passage of high-temperature brine (Oudin et al., 1984; Ramboz et al., 1988). Because of high temperature, incoming hydrothermal fluid can have a higher H_2S/dissolved metal ratio than the lower brine pool. Vertical advection of a more sulphide-rich fluid through the sediments would be expected to produce the profiles observed for core 683, with unit L, which was most affected by inflowing hydrothermal fluid, showing the lowest metal values. Metals precipitate as sulphide minerals in veins (Pottorf and Barnes, 1983; Zierenberg and Shanks, 1988; Missack et al., 1989). One would also expect that the least soluble sulphides (Cu, Cd) would show greater depletion than the more soluble sulphide (Fe, Zn) (Barnes, 1979), as observed.

Core 684 presents another major difference compared with core 683. It contains Mn-oxides, which are strong oxidizing agent for Fe^{2+} (Stumm and Morgan, 1996). The redox reaction produces dissolved Mn^{2+}, and Fe^{2+} is oxidized and precipitates as a Fe(III) phase. Mn-oxides have been detected in unit 3, between 10 m and 8.75 m, and between 6 m and 4.15 m. The diagenetic redox reactions linked to the presence of Mn-oxides can produce the profiles observed for core 684. The concentration of dissolved Fe drops to low values in these layers and the concentration of Mn is the highest in unit 3. Therefore, some iron oxides probably precipitate nowadays at the expense of the Mn-oxides precipitated a few thousand years ago. This reaction can support a downward diffusive flux of dissolved Fe from the upper brine to the unit 3, and may represent a sink for dissolved Fe(II).

The concentration of dissolved Mn decreases abruptly above the layer that contains Mn-oxides. This suggests that Mn^{2+} is trapped again in the solid fraction. The top of unit 3, which is depleted in Mn-oxides, contains effectively up to 13 wt.% Mn(II) mineral present as rhodocrosite ($MnCO_3$) and Mn, Fe, and Ca-carbonate solid solution. This suggests that Mn-carbonates are of diagenetic origin and that they control the dissolved Mn^{2+} concentration. Core 683 contains no Mn-oxides. This may explain the relatively constant concentration of dissolved manganese in this core.

The interstitial waters collected in the Mn and Fe-oxide-rich

sediment from unit 3 in core 684 show small peaks of Zn, Cu, and Cd-concentrations. We suggest that these maxima result from the recrystallization during diagenesis of oxide minerals that originally settled. The Mn(III,IV) and Fe(III) minerals which have been identified by X-ray diffraction in the unit 3 mostly consist of goethite, haematite, manganite, or todorokite. The primary precipitates are amorphous hydroxides that form at the redox boundaries above the lower brine (Bischoff, 1969; Danielsson et al., 1980; Hartmann, 1985; Anschutz, 1993), which undergo diagenetic recristallization to more stable forms after settling. The primary precipitate of Fe(III) phase is ferrihydrite, which is present at the top of the cores (Badaut, 1988). Several studies have shown that ferrihydrite can form goethite and haematite, depending on environmental conditions (e.g., Chruckrov et al., 1979; Murray, 1979; Fischer and Schwertmann, 1975; Schwertmann and Murad, 1983; Cornell, 1988). The transfomation of primary Mn-oxides to more stable minerals, such as manganite or todorokite has been observed in experiments (Giovanoli et al., 1976; Hem and Lind, 1983). The adsorption capacity of the oxide minerals in the sediment must be lower than that of the amorphous particles that precipitated above because of decreased surface-to-volume ratio. Therefore, the specific surface available for adsorption is lower in the sediment compared to the initial particles, and the trace elements can be released in pore waters.

5. CONCLUSIONS

Generally Cl is conservative in marine sediment pore waters. We showed that the dissolved major elements of the Atlantis II Deep, such as Na and Cl, did not have a conservative behaviour, because they were controlled in some layers by equilibrium with a solid salt. Major element concentrations in pore waters of Atlantis II Deep sediments show small variations between the two studied cores and along the sedimentary columns. We have calculated that the pore waters are undersaturated with respect to halite for the in situ conditions, but this is an artifact due to the re-equilibration of the pore waters for the shipboard conditions. Such an artifact must have occurred for all the previous studies of pore water salinity of the Atlantis II Deep cores. Therefore, even if the measured TDS of the interstitial brines is uniform in core 684, in fact, there is probably a salinity gradient in situ, between the bottom of the core, which contains halite, and the upper units, which have chloride and sodium concentrations below saturation with respect to halite. The presence of halite in both cores suggests that the dissolved salt content of the deep was higher in the past than that corresponding to the saturation at 220 bars and 62°C, i.e., the Atlantis II deep was filled with warmer brines. The transient model of salt transport shows that the pore water cannot record the chemistry of buried waters. For example, we calculated that the pore water record of modern variation of brine salinity is rapidly smoothed by molecular diffusion.

The shape of the dissolved metal profiles in core 683 can be explained by advection of hydrothermal fluids through the sediment, which agrees with the metasomatic effects observed in the sediment of the SW basin. The dissolved metal profiles of core 684 mostly reflect diagenetic reactions. The manganese oxide layers of unit 3 represent a sink for dissolved Fe^{2+}, which can diffuse into this unit from the overlying brine. Fe^{2+}

is oxidised and precipitated in the presence of Mn-oxides. The Mn^{2+} that is produced during this reaction may not diffuse to the brine pool if there is sufficient carbonate available for it to precipitate as Mn-carbonate. The recrystallization of iron and manganese oxides causes the partial desorption of trace metals, which become enriched in pore waters of unit 3.

REFERENCES

Anschutz P. (1993). Genèse et évolution géochimique des sédiments métallifères de la fosse Atlantis II (mer Rouge). PhD Thesis, Univ. Louis Pasteur.

Anschutz P. and Blanc G. (1993a) Le rapport NaCl/eau des boues minéralisées de la fosse Atlantis II (mer Rouge). Calcul de la teneur en halite des sédiments et implication sur la paléotempérature du milieu. *C.R. Acad. Sci. Paris* **317,** 1595–1600.

Anschutz P. and Blanc G. (1993b) L'histoire sédimentologique de la fosse Atlantis II (mer Rouge). Les apports de la micropaléontologie. *C.R. Acad. Sci. Paris* **317,** 1303–1308.

Anschutz P. and Blanc G. (1995a) Chemical mass balances in metalliferous deposits from the Atlantis II Deep (Red Sea). *Geochim. Cosmochim. Acta* **59,** 4205–4218.

Anschutz P. and Blanc G. (1995b) Geochemical dynamics of the Atlantis II Deep (Red Sea): Silica behavior. *Mar. Geol.* **128,** 25–36.

Anschutz P. and Blanc G. (1996) Heat and salt fluxes in the Atlantis II Deep (Red Sea). *Earth Planet. Sci. Lett.* **142,** 147–159.

Anschutz P., Blanc G., and Stille P. (1995) Origin of fluids and the evolution of the Atlantis II Deep hydrothermal system (Red Sea): Sr isotope study. *Geochim. Cosmochim. Acta* **59,** 4799–4808.

Anschutz P., Turner J. S., and Blanc G. (1998) The development of layering, fluxes through double-diffusive interfaces, and location of hydrothermal sources of brines in the Atlantis II Deep: Red Sea. *J. Geophys. Res.* **103,** C12, 27809–27819.

Anschutz P., Blanc G., Chatin F., Geiller M., and Pierret M.-C. (1999) Hydrographic changes during 20 years in the brine-filled basins of the Red Sea. *Deep Sea Res. Part I* **46,** 1779–1792.

Bäcker H. and Richter H. (1973) Die rezente hydrothermal-sedimentäre Lagerstätte Atlantis II Tief im Roten Meer. *Geol. Rundsch.* **62,** 697–741.

Badaut D. (1988) Les argiles et les composés silico-ferriques des sédiments métallifères de la fosse Atlantis II (Mer Rouge). Formation et diagenèse des dépôts. Thesis Doc. ès Sci., Univ. Paris Sud.

Badaut D., Blanc G., and Decarreau A. (1990) Variation des minéraux argileux ferrifères, en fonction du temps et de l'espace, dans les dépôts métallifères de la fosse Atlantis II en Mer Rouge. *C.R. Acad. Sci. Paris* **310,** 1069–1075.

Badaut D., Decarreau A., and Besson G. (1992) Feripyrophyllite and related Fe^{3+}-rich 2:1 clays in recent deposits of Atlantis II Deep, Red Sea. *Clay Miner.* **27,** 389–404.

Barnes H. L. (1979) Solubilities of ore minerals. In *Geochemistry of Hydrothermal Ore Deposits* (ed. H. L. Barnes), pp. 404–460. Wiley–Interscience.

Berner R. A. (1980) *Early Diagenesis: A Theoretical Approach.* Princeton Univ. Press.

Bischoff J. L. (1969) Red Sea geothermal brine deposits: Their mineralogy, chemistry, and genesis. In *Hot Brines and Recent Heavy Metal Deposits in the Red Sea* (eds. E. T. Degens and A. D. Ross), pp. 368–401. Springer Verlag.

Bischoff J. L. (1972) A ferroan nontronite from the Red Sea geothermal system. *Clays Clay Min.* **20,** 217–223.

Blanc G. (1987) Géochimie de la fosse Atlantis II (Mer Rouge). Evolution spatio-temporelle et rôle de l'hydrothermalisme. PhD thesis, Univ. Pierre et Marie Curie.

Blanc G. and Anschutz P. (1995) New hydrographic situation in the Atlantis II Deep hydrothermal brine system. *Geology* **23,** 543–546.

Blanc G., Boulègue J., Badaut D., and Stouff P. (1986) Premiers résultats de la campagne océanographique Hydrotherm (Mai 85) du Marion-Dufresne sur la fosse Atlantis II (Mer Rouge). *C.R. Acad. Sci. Paris* **302,** 175–180.

Blanc G., Boulègue J., and Charlou J. L. (1990) Profils d'hydrocarbures légers dans l'eau de mer, les saumures et les eaux interstitielles de la fosse Atlantis II (mer Rouge). *Oceanologica Acta* **13,** 187–197.

Blanc G., Boulègue J., and Michard A. (1995) Isotope compositions of the Red Sea hydrothermal end-member. *C.R. Acad. Sci. Paris* **320,** 1187–1193.

Blanc G., Anschutz P., and Pierret M.C. (1998) Metalliferous sedimentation into the Atlantis II Deep: A geochemical insight. In *Sedimentation and Tectonics of Rift Basins: Red Sea-Gulf of Aden* (eds. B. H. Purser and D. W. J. Bosence), pp. 505–520. Chapman & Hall.

Boudreau B. P. (1996) The diffusive tortuosity of fine-grained unlithified sediments. *Geochim. Cosmochim. Acta* **60,** 3139–3142.

Brewer P. G. and Spencer P. G. (1969) A note on the chemical composition of the Red Sea brines. In *Hot Brines and Recent Heavy Metal Deposits in the Red Sea* (eds. E. T. Degens and A. D. Ross), pp. 174–179. Springer Verlag.

Brooks R. R., Kaplan I. R., and Peterson M. N. A. (1969) Trace element composition of Red Sea geothermal brine and interstitial water. In *Hot Brines and Recent Heavy Metal Deposits in the Red Sea* (eds. E. T. Degens and A. D. Ross), pp. 180–203. Springer Verlag.

Chuckrov F. V., Zvyagin B. B., Gorskhov A. I., Yermilova L. P., and Balaskova V. V. (1973) Ferrihydrite. *Izvest. Intern. Geol. Rev.* **16,** 1131–1143.

Cornell R. M. (1988) The influence of some divalent cations on the transformation of ferrihydrite to more cristalline products. *Clay Min.* **23,** 329–332.

Danielsson L. G., Dyrssen D., and Graneli A. (1980) Chemical investigations of Atlantis II and Discovery brines in the Red Sea. *Geochim. Cosmochim. Acta* **44,** 2051–2065.

Dupré B., Blanc G., Boulègue J., and Allègre C. J. (1988) Metal remobilization at a spreading centre studied using lead isotopes. *Nature* **333,** 165–167.

Erickson A. J. and Simmons G. (1969) Thermal measurement in the Red Sea hot brine pools. In *Hot Brines and Recent Heavy Metal Deposits in the Red Sea* (eds. E. T. Degens and A. D. Ross), pp. 114–121. Springer Verlag.

Giovanoli R., Feitknecht W., Maurer R. and Häne H. (1976) Über die Reaktion von Mn_3O_4 mit Säuren. *Chimica* **30,** 307–309.

Felmy A. R. and Weare J. H. (1991) Calculation of multicomponent ionic diffusion from zero to high concentration: I. Na-K-Ca-Mg-Cl-SO_4-H_2O at 25°C. *Geochim. Cosmochim. Acta* **55,** 113–131.

Fischer W. R. and Schwertmann U. (1975) The formation of hematite from amorphous iron(III) hydroxide. *Clays Clay Min.* **23,** 33–37.

Hackett J. and Bischoff J. L. (1973) New data on the stratigraphy, extent, and geologic history of the Red Sea geothermal deposits. *Econ. Geol.* **68,** 553–564.

Hartmann M. (1973) Untersuchung von suspendiertem Material in den Hydrothermal-Laugen des Atlantis II Tiefs. *Geol. Rundsch.* **62,** 742–754.

Hartmann M. (1985) Atlantis II deep geothermal brine system. Chemical processes between hydrothermal brines and Red Sea deep water. *Mar. Geol.* **64,** 157–177.

Hartmann M., Scholten J. C., and Stoffers P. (1998) Hydrographic structure of brine filled deeps in the Red Sea. Correction of the Atlantis II Deep temperatures. *Mar. Geol.* **144,** 331–332.

Hem J. D. and Lind C. J. (1983) Nonequilibrium models for predicting forms of precipitated manganese oxides. *Geochim. Cosmochim. Acta* **47,** 2037–2046.

Hendricks R. L., Reisbick F. B., Mathaffey E. J., Roberts D. B., and Peterson M. N. A. (1969) Chemical composition of sediments and interstitial brines from the Atlantis II, Discovery and Chain deeps. In *Hot Brines and Recent Heavy Metal Deposits in the Red Sea* (eds. E. T. Degens and A. D. Ross), pp. 407–440. Springer Verlag.

Ku T. L., Thurber D. L., and Mathieu G. G. (1969) Radiocarbon chronology of Red Sea sediments. In *Hot Brines and Recent Heavy Metal Deposits in the Red Sea* (eds. E. T. Degens and A. D. Ross), pp. 348–359. Springer Verlag.

Lasaga A. C. (1979) The traitment of multicomponent diffusion and ion pairs in diagenetic fluxes. *Am. J. Sci.* **279,** 324–346.

Lerman A. and Jones B. F. (1973) Transient and steady-state salt transport between sediments and brine in closed lakes. *Limnol. Oceanogr.* **18,** 72–85.

Li Y. H. and Gregory S. (1974) Diffusion of ions in seawater and in deep-sea sediments. *Geochim. Cosmochim. Acta* **38,** 703–714.

Manheim F. T., Waterman L. S., Woo C. C., and Sayles F. L. (1974) Interstitial water studies on small core samples, Leg 23 (Red Sea). In *Init. Repts. DSDP*, 23, (eds. Whitmarsh R. B., Weser D. E., Ross D. A., et al.), pp. 955–967. U.S. Gov. Printing Office.

Middelburg J. J. and DeLange G. J. (1989) The isolation of Kau Bay during the last glaciation: Direct evidence from interstitial water chlorinity. *Nether. J. Sea Res.* **24,** 615–622.

Missack E., Stoffers P., and El Goresy A. (1989) Mineralogy, paragenesis, and phases relations of copper iron sulfides in the Atlantis II Deep, Red Sea. *Min. Deposita* **24,** 82–91.

Monnin C. (1994) Density calculation and concentration scale conversions for natural waters. *Computer Geosci.* **20,** 1435–1445.

Monnin C. (1999) A thermodynamic model for the solubility of barite and celestite in electrolyte solutions and seawater to 200°C and to 1 kbar. *Chem. Geol.* **153,** 187–209.

Monnin C. and Ramboz C. (1996) The anhydrite saturation index of the Red Sea ponded brines and sediment pore waters of the Red Sea deeps. *Chem. Geol.* **127,** 141–159.

Murray J. W. (1979) Iron oxides. In *Marine Minerals* (ed. P. J. Ribbe), pp. 47–98. Am. Mineral. Soc.

Oudin E., Thisse Y., and Ramboz C. (1984) Fluid inclusion and mineralogical evidence for high temperature saline hydrothermal circulation in the Red Sea metalliferous sediments:preliminary results. *Mar. Mining* **5,** 3–31.

Pottorf R. J., and Barnes H. L. (1983) Mineralogy, geochemistry, and ore genesis of hydrothermal sediments from Atlantis II Deep, Red Sea. *Econ. Geol. Monogr.* **5,** 198–223.

Pushkina Z. V., Stepanets M. I., Orlora L. P., and Simani T. I. (1982) Fe, Mn, Cu, Co, Ni, Zn, Pb, Cd, B and Si in the interstitial waters of the metalliferous sediments in the Red Sea (Atlantis II and Discovery Deeps). *Geochem. Int.* **1982,** 587–593.

Ramboz C., Oudin E. and Thisse Y. (1988) Geyser-type discharge in Atlantis II Deep, Red Sea: Evidence of boiling from fluid inclusions in epigenetic anhydrite. *Can. Mineral.* **26,** 765–786.

Reeburgh W. S. (1967) An improved interstitial water sampler. *Limnol. Oceanogr.* **12,** 163–165.

Schwertmann U., Friedl J., Stanjek H., Murad E., and Bender Koch C. (1998) Iron oxides and smectites in the sediments from the Atlantis II Deep, Red Sea. *Eur. J. Min.* **10,** 953–967.

Schwertmann U. and Murad E. (1983) Effect of pH on the formation of goethite and hematite from ferrihydrite. *Clays Clay Min.* **31,** 277–284.

Shanks W. L. III and Bischoff J. L. (1980) Geochemistry, sulfur isotope composition and accumulation rates of the Red Sea geothermal deposits. *Econ. Geol.* **75,** 445–459.

Stumm W. and Morgan J. J. (1996) *Aquatic Chemistry, 3rd Ed.* Wiley.

Turner J. S. (1969) A physical interpretation of the observations of the hot brine layers in the Red Sea. In *Hot Brines and Recent Heavy Metal Deposits in the Red Sea* (eds. E. T. Degens and A. D. Ross), pp. 164–173. Springer Verlag.

Urvois M. (1988) Apports de l'estimation géostatistique de l'épaisseur des unités métallifères dans la compréhension des mécanismes de mise en place des sédiments de la fosse Atlantis II (Mer Rouge). *Doc. BRGM* 154.

VonDamm K. L. (1990) Seafloor hydrothermal activity:Black smoker chemistry and chimneys. *Ann. Rev. Earth Planet Sci.* **18,** 173–204.

Voorhis A. D. and Dorson D. L. (1975) Thermal convection in the Atlantis II hot brine pool. *Deep-Sea Res.* **22,** 167–175.

Zierenberg R. A. and Shanks W. C. III (1983) Mineralogy and geochemistry of epigenetic metalliferous sediments, Atlantis II Deep, Red Sea. *Econ. Geol.* **78,** 57–72.

Zierenberg R. A. and Shanks W. C. III (1986) Isotopic variations on the origin of the Atlantis II, Suakin and Valdivia brines, Red Sea. *Geochim. Cosmochim. Acta* **50,** 2205–2214.

Zierenberg R. A. and Shanks W. C. III (1988) Isotopic studies of epigenetic features in metalliferous sediments, Atlantis II deep, Red Sea. *Can. Min.* **26,** 737–753.